Desalination and Water Treatment
www.deswater.com
doi: 10.1080/19443994.2015.1027281

57 (2016) 8884–8893
April

Taylor & Francis
Taylor & Francis Group

Removal of methyl violet dye by adsorption onto mesoporous mixed oxides of cerium and aluminum

Piaw Phatai[a,*], Cybelle Morales Futalan[b]

[a]*Faculty of Science, Department of Chemistry, Udon Thani Rajabhat University, Udon Thani 41000, Thailand, Tel. +66 42 211 040, ext. 201-3; Fax: +66 42 341 614 5; email: piawtee99@hotmail.com*
[b]*Operations Department, Frontier Oil Corporation, Makati 1229, Philippines, Tel. +63 24 785 854; Fax: +63 28 172 755; email: cmfutalan@gmail.com*

Received 1 December 2014; Accepted 2 March 2015

ABSTRACT

In this study, the adsorption efficiency of methyl violet dye onto Ce03Al07, Ce05Al05, and Ce07Al03 mixed oxides was investigated. The properties of Ce/Al oxides were determined by scanning electron microscope, X-ray diffraction, FT-Raman spectrometry, and N_2 adsorption–desorption isotherms. Characterization tests showed that synthesized Ce/Al oxide with fluorite has pure cubic structure of mesoporous nature and non-uniform in size with rough surface. Moreover, the surface areas of Ce/Al oxides were observed to decrease with increase in cerium content. The batch adsorption experiments were performed at 25°C and various parameters including solution pH, contact time, and initial dye concentration were studied. The dye adsorption of Ce03Al07 mixed oxide attained equilibrium at 15 min, which was faster than that of Ce05Al05 and Ce07Al03. The equilibrium adsorption data were analyzed using Langmuir, Freundlich, and Temkin isotherms. The adsorption behavior of methyl violet onto Ce03Al07 (R^2 = 0.9739) was found to follow the Langmuir isotherm, providing maximum monolayer adsorptive capacity of 25 mg/g. On the other hand, the adsorption of methyl violet onto Ce05Al05 (R^2 = 0.9581) and Ce07Al03 (R^2 = 0.9894) followed the Freundlich isotherm.

Keywords: Cerium and aluminum mixed oxides; Langmuir isotherm; Methyl violet dye; Temkin isotherm

1. Introduction

Methyl violet (MV) dye, $C_{24}H_{28}ClN_3$, is a mixture of hexamethyl, pararosanilines, pentamethyl, and tetramethyl. The dye is commonly known as crystal violet or methyl violet 10B [1]. It is a triphenylmethane powdered dye with dark green color that has a poor resistance toward light and chemical bleaches and is soluble in water, ethanol, diethylene glycol, dipropylene glycol, and methanol [2]. Common uses of MV dye are as pH indicator in analytical laboratories; dyeing of bamboo, cotton, leather, paper, silk, and straw; and heterography and printing inks. Moreover, MV dye is naturally present in the effluent of several industries, such as the textile, cosmetic, plastic, paper, printing, and pharmaceutical industries and is routinely discharged into natural streams and rivers. The presence of MV dye in surface waters and groundwater can cause significant problems to public

*Corresponding author.

health such as irritation in eyes, gastrointestinal tract, skin, and respiratory tract [1]. MV is a mutagen, mitotic poison, and clastogen [3] and was reported to be potentially carcinogenic [4]. In addition, dyes reduce the penetration of light that leads to disruption of the biological metabolism processes that can cause destruction of aquatic communities [5–7].

Several technologies are available for the removal of MV dye in waters including chemical oxidation, froth flotation, adsorption, coagulation, phytoextraction, ultrafiltration, reverse osmosis, and electrodialysis. Among these, adsorption has been considered to be an attractive method because it has several advantages such as high efficiency, ease of operation, low cost, simplicity of design, and profitability [8–10]. Adsorption has been extensively studied for the removal of various contaminants such as color, dyes, heavy metals, and phenols using nanoalumina, egg shell wastes, egg shell membrane, hen feather, bottom ash, and *Hibiscus cannabinus* fiber grafted with vinyl monomer acrylic acid [11–18]. The removal of MV dye concentration from aqueous solution has been widely investigated, where previous researches include adsorbents such as stevensite-rich clay [19], granulated activated carbon [20], bagasse fly ash [21], mansonia wood sawdust [22], sepiolite [23], cellulose [24], peach gum [25], and nanographite/Fe_3O_4 [26]. Recently, researchers have intensified their efforts in exploring the use of metal ion-based oxides as an adsorbent for the removal of contaminants in wastewater. Mixed metal oxides, such as Fe–Sn oxide for fluoride removal [27], Ni–Zn oxide for methyl orange and tartrazine removal [28], and Fe–Mn mixed oxide for selenium removal [29], have been investigated. Mixed oxides have desirable properties, such as high surface area and small crystallite size, which would have a significant impact upon the adsorption process. Accordingly, there has been increased attention devoted to the development of new adsorbent materials with various compositions and properties.

The purpose of the present study is to investigate the adsorption capacity of Ce03Al07, Ce05Al05, and Ce07Al03 for the removal of MV dye from aqueous solution. The effect of different experimental conditions, such as Ce/Al molar ratio, solution pH, contact time, and initial dye concentration, on the removal efficiency and adsorption capacity was examined. The properties of the Ce/Al mixed oxides were determined by scanning electron microscope (SEM), X-ray diffraction (XRD), FT-Raman spectrometry and N_2 adsorption–desorption isotherms. Isotherm models such as Langmuir, Freundlich, and Temkin were utilized to determine the adsorption phenomena information which may be useful for further research and practical applications of the adsorbent in dye wastewater treatment.

2. Materials and methods

2.1. Materials

Chemical reagents such as $Ce(NO_3)_3{\cdot}6H_2O$, $Al(NO_3)_3{\cdot}6H_2O$, ethylene glycol 20,000, NH_4OH, n-C_4H_9OH, KH_2PO_4, KOH, $NaH_2PO_4{\cdot}H_2O$, Na_2HPO_4, H_3PO_4, H_3BO_3, and NaOH were purchased from Merck (Germany). The MV was used without additional purification, and its chemical structure is shown in Fig. 1. Stock solutions of MV dye were prepared by dissolving weighed amounts of MV with deionized water. Buffer solutions of various pH ranges from 3 to 9 were prepared (European Pharmacopoeia 5.0, 2012). All chemicals were of analytical grade and utilized without further purification.

2.2. Preparation of adsorbent

The preparation of Ce_xAl_{1-x} mixed oxides (x = 0.3, 0.5, and 0.7) was carried out using a modified co-precipitation methodology similar to that of Chen et al. [30]. The molar ratio composition of Ce_xAl_{1-x} mixed oxides was varied: $Ce_{0.3}Al_{0.7}$, $Ce_{0.5}Al_{0.5}$, and $Ce_{0.7}Al_{0.3}$ that would be referred to as Ce03Al07, Ce05Al05, and Ce07Al03, respectively. A mixture of $Ce(NO_3)_3{\cdot}6H_2O$ and $Al(NO_3)_3{\cdot}9H_2O$ at the desired molar ratios was dissolved in water and NH_4OH. About 1.0 g of ethylene glycol 20,000 was slowly added into the mixture under vigorous stirring until a pH of 9.0 is attained. Then, the solution was frozen for 24 h at 0℃, and the resulting gel was filtered. Next, the purple gel was cleaned with n-butyl alcohol repeatedly. After several

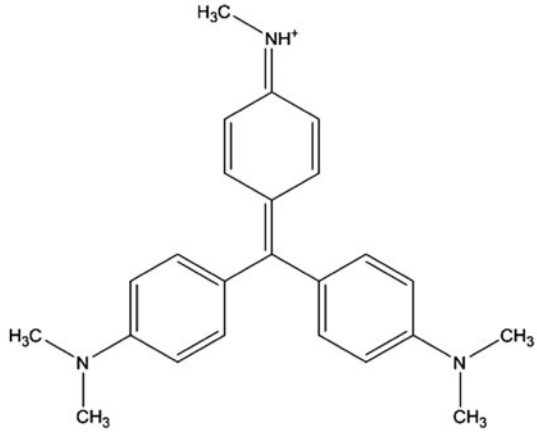

Fig. 1. Structure of methyl violet dye.

washings, the samples were dried at 120˚C for 2 h and the resulting powder was calcined in air at 600˚C for 4 h.

2.3. Equipment

All pH measurements were performed using a pH meter (Consort C830, Belgium). An electronic balance (Precisa XB220A) with an accuracy of 0.0001 g was used for weighing the adsorbent and chemicals. The dye concentrations were measured using the absorbance over wavelength of 584 nm and were recorded in a UV–vis spectrophotometer (Spectronics Genesis 2).

The morphology and surface structure of the Ce/Al mixed oxide were determined by scanning electron microscope (SEM, JEOL-JPM-6010LV) with an accelerating voltage of 10 kV. Crystal phases of Ce/Al mixed oxides were analyzed using a X-ray diffractometer (XRD, Bruker D2 Phaser) with an accelerating voltage of 30 kV, current of 10 mA, and Cu Kα radiation (λ = 1.5405 Å). The Raman spectrum was generated using a V70-RAM II FT-Raman Spectrometer in the range of 1,500–200 cm^{-1} with spectral resolution of 1 cm^{-1}. The N_2 adsorption–desorption isotherms were determined using Quantachrome AUTOSORB-1. The physical properties of the Ce/Al mixed oxides that include specific surface area and average pore diameter were calculated using the Brunauer, Emmett, and Teller method from adsorption data with a relative pressure range of 0.01–0.99. The pore size distribution and total pore volume were determined by the Barrett–Joyner–Halenda method.

2.4. Batch adsorption studies

All batch adsorption experiments were performed using a 250-mL Erlenmeyer flask in an orbital shaker bath (VS-202P, AC220 V, 50 Hz). In a typical batch experiment, about 0.1 g adsorbent was placed in an Erlenmeyer flask with 25 mL of dye solution and agitated at a constant speed of 150 rpm. The effect of varying parameters such as contact time (15–120 min), solution pH (3–9), and initial dye concentration (25–200 mg/L) on the removal efficiency and adsorption capacity was evaluated. After reaching equilibrium, the mixture was filtered with Whatman-42 filter paper to determine the residue concentrations. The residual MV dye in the filtrate was diluted and analyzed by UV–vis spectrophotometer at a maximum wavelength of 584 nm. All the batch experiments were repeated three times to optimize precision of the results.

2.5. Isotherm studies

Equilibrium studies were performed by agitating 0.1 g Ce/Al mixed oxides and 25 mL of solution (pH 9.0) at 150 rpm for 120 min at 25˚C. The isotherm study was carried out by varying the initial MV concentration from 25 to 200 mg/L.

3. Results and discussion

3.1. Characterization of Ce/Al mixed oxide

In Fig. 2, the SEM images of the Ce03Al07 mixed oxide at 3,000× and 4,500× magnifications are shown. The Ce03Al07 mixed oxides are illustrated as blocks with non-uniform sizes and rough surfaces. However, the porosity of the oxide could not be seen from the micrographs.

The XRD patterns of Ce03Al07, Ce05Al05, and Ce07Al03, calcined at 600˚C for 4 h, are shown in Fig. 3. For all three adsorbents, the XRD patterns illustrate four main peaks located at 28˚, 32˚, 47˚, and 55˚. Moreover, two smaller peaks located at 69˚ and 76˚ were observed. These diffraction peaks are characteristic of a pure cubic structure of CeO_2 with fluorite (JCPDS 34-394). The major peak of CeO_2 is located at

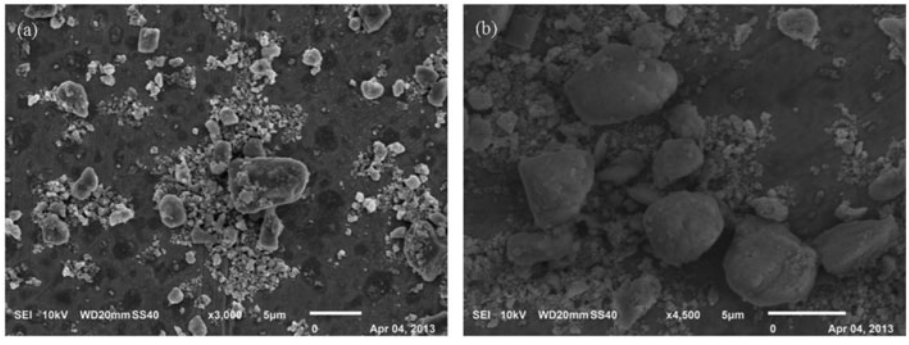

Fig. 2. SEM micrographs of Ce03Al07 mixed oxides at (a) 3,000× and (b) 4,500× magnifications.

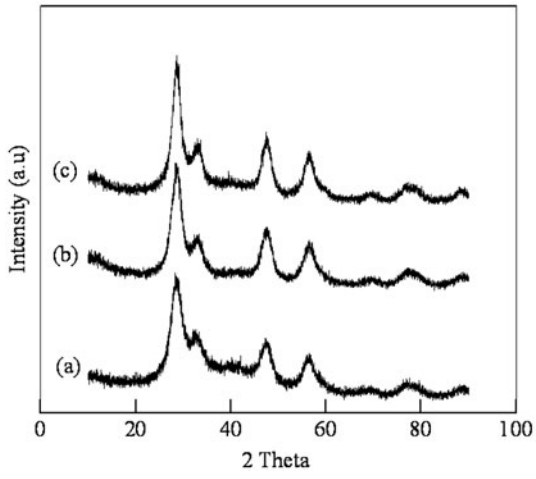

Fig. 3. XRD patterns of (a) Ce03Al07, (b) Ce05Al05, and (c) Ce07Al03.

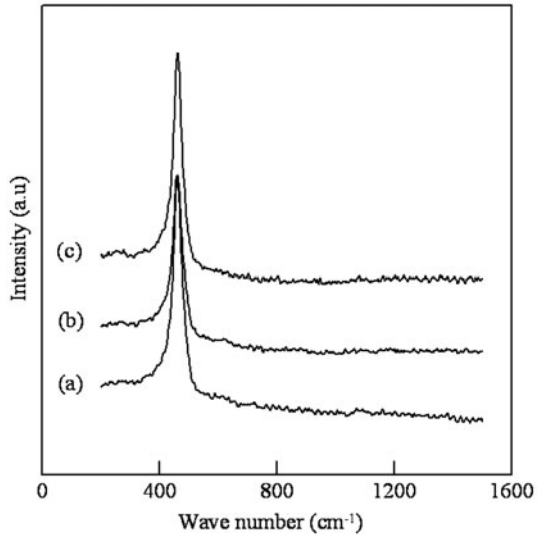

Fig. 4. Raman spectra of (a) Ce03Al07, (b) Ce05Al05, and (c) Ce07Al03.

$2\theta = 28^{\circ}$, which is attributed to the [1 1 1] lattice plane of the face-centered cubic of CeO_2 [31]. There are no peaks for Al_2O_3 observed in the XRD patterns. It is observed that increasing the amount of Al^{3+} in the mixed oxides causes broadening of the peaks due to lattice strain caused by the insertion of Al^{3+} into the crystal structure of CeO_2. The insertion of Al^{3+} is due to the smaller ionic radius of Al^{3+} (0.054 nm) compared to Ce^{4+} (0.101 nm) at the 6-coordinate configuration.

The Raman spectroscopy validates the formation of CeO_2 particles, where the spectra of Ce/Al mixed oxides are illustrated (Fig. 4). In all Raman spectra, a strong band at 464.5 cm^{-1} is observed that could be attributed to the F_2 g symmetrical breathing mode of O atoms around each cerium ion [32,33]. Moreover, the vibrational mode is almost independent of the ionic mass of cerium because the only movement is attributed to O atoms. There is no effect on the fluorite structure, even if the Ce–Al ratio was varied. In addition, the absence of hydrous metal oxides could be attributed to the calcination at 600˚C for 4 h. A previous study by Liu et al. [34] prepared an Al–Ce hybrid adsorbent via the co-precipitation method (without calcination) for the removal of fluoride ions in drinking water. Therefore, the hydroxyl functional group of the metal oxide (M-OH), a crucial requirement for the adsorption of fluoride ions in water, was present in the hybrid adsorbent [34].

Fig. 5 illustrates the N_2 adsorption–desorption isotherms and corresponding pore size distribution curves for Ce03Al07, Ce05Al05, and Ce07Al03, and their textural properties are listed in Table 1. Based on the IUPAC classification, the isotherms of all samples have large hysteresis loops and correspond to a typical IV isotherm, which are characteristics of mesoporous materials [35,36]. The pore size distribution curves of Ce03Al07 and Ce05Al05 present a bimodal structure, which shows a narrow peak at ~3 nm and broad peak at ~7 nm. Meanwhile, Ce07Al03 has only one broad peak located at 5 nm. The pore size distribution curves suggest that Ce03Al07, Ce05Al05, and Ce07Al03 have an average pore diameter ranging between 5 and 7 nm. From Table 1, the specific surface area and total pore volume of the samples were observed to decrease as the cerium content in the mixed oxides was increased, which is attributed to the accumulation of CeO_2 within the adsorbent pores [37].

3.2. Effect of solution pH

Solution pH is an important determinant of dye adsorption from aqueous solution, as it affects the concentration of the counter ions on the adsorbent and degree of ionization of the adsorbate during adsorption. As shown in Fig. 6, the percentage removal of MV dye increases as the solution pH was increased from 3.0 to 9.0. The low removal efficiency at acidic pH is due to positive surface charge of Ce/Al oxides, which creates an electrostatic repulsion between active sites on the adsorbent and cationic dye. Moreover, a competition between H^+ and MV dye molecules for the adsorption sites would cause further decrease in removal efficiency. On the other hand, the adsorbents would acquire a net negative surface charge at alkaline pH. This indicates an enhanced affinity between the

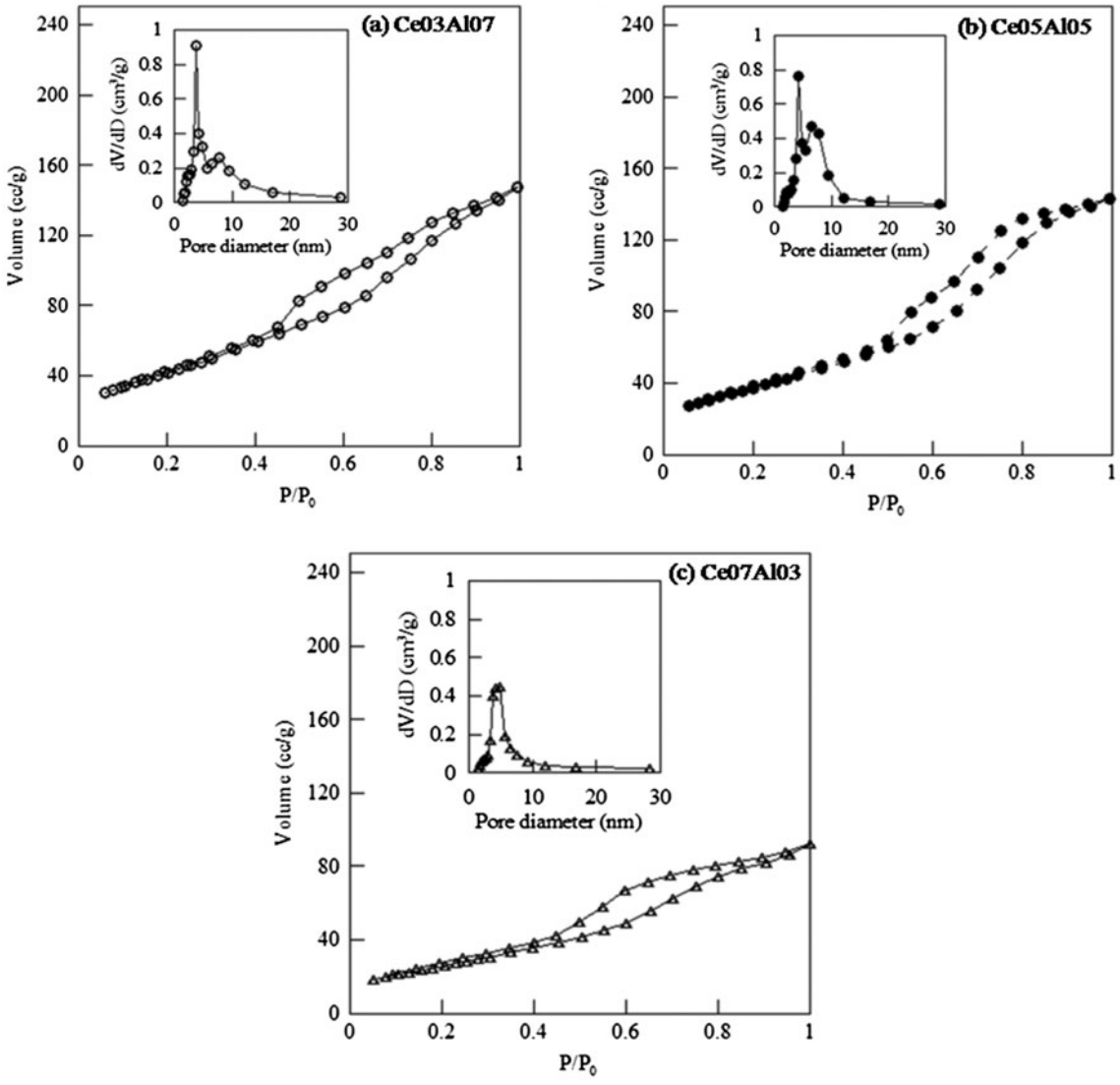

Fig. 5. N_2 adsorption–desorption profiles and pore size distribution of Ce/Al mixed oxide adsorbents; (a) Ce03Al07, (b) Ce05Al05, and (c) Ce07Al03.

Table 1
Textural properties of Ce03Al07, Ce05Al05, and Ce07Al03 derived from N_2 adsorption–desorption isotherms

Adsorbents	Specific surface area (m^2/g)	Total volume (cm^3/g)	Average pore diameter (nm)
Ce03Al07	158	0.22	5.75
Ce05Al05	141	0.22	6.30
Ce07Al03	97	0.14	5.94

cationic MV molecules and adsorbent through electrostatic forces of attraction, which would result to an increase in the removal efficiency. As the overall graph indicates that maximum MV dye uptake occurs at pH 9.0 for Ce03Al07, Ce05Al05, and Ce07Al03, therefore subsequent studies were conducted at this pH value. A similar trend was observed, where the maximum MV adsorption using wood sawdust [38], biochar [39], and bagasse fly ash [21] occurred at pH 9.

3.3. Effect of contact time

To establish the equilibrium time for maximum adsorption, experiments were conducted under different contact times ranging from 15 to 120 min (Fig. 7). For the adsorption of MV dye, a rapid uptake was observed during the initial contact time. For the first

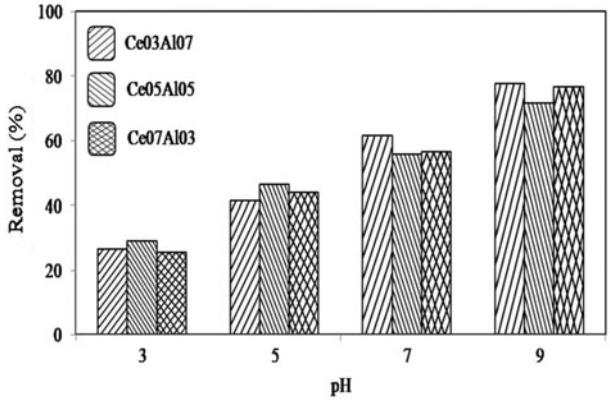

Fig. 6. Effect of solution pH on removal efficiency of MV dyes by Ce/Al mixed oxides (adsorbent dose = 0.10 g; initial dye concentration = 10 mg/L).

15 min, an instantaneous external adsorption occurs due to a high number of adsorption sites available for binding [40,41]. At 30 min, the uptake of Ce/Al oxides was observed to slow down gradually until equilibrium is attained at about 120 min. When the adsorption process approaches equilibrium, the sites on the adsorbent are almost covered by MV molecules. The remaining binding sites on the surface become more difficult to be filled in due to the repulsive forces existing between the MV molecules on the adsorbent and unbound MV molecules in the bulk phase. Previous studies showed that other adsorbents such as *Phragmites australis* activated carbon and bagasse fly ash have longer equilibrium time of 150 and 240 min, respectively [21,42].

3.4. Effect of initial dye concentration

The effect of initial concentrations on the removal percentage of MV dye using Ce03Al07, Ce05Al05, and Ce07Al03 is illustrated in Fig. 8. It is observed that the percentage removal of Ce03Al07 decreases from 93.45 to 75.67% with increasing initial dye concentration from 25 to 200 mg/L. This is due to the saturation of active sites of Ce03Al07 at high concentrations of MV dye. The results obtained from this study are in agreement with previous studies of Ghorai et al. [43] and Chen et al. [42]. The same trend was observed for the removal of MV dye using polyacrylamide grafted xanthan gum and incorporated nanosilica and activated carbon derived from *P. australis* [42,43]. However, the adsorption of MV dye onto Ce05Al05 and Ce07Al03 shows an opposite trend, where a gradual increase in the removal efficiency was observed with increasing dye concentration. This is due to the greater average

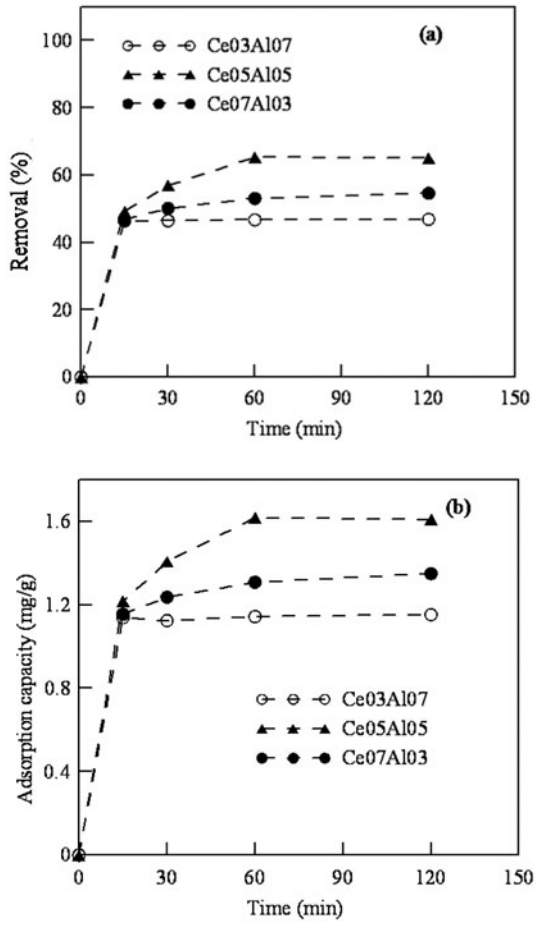

Fig. 7. The effect of contact time on (a) percentage adsorption of MV dyes and (b) adsorption capacity by Ce/Al mixed oxides (adsorbent dose = 0.10 g; initial dye concentration = 10 mg/L; pH 9.0).

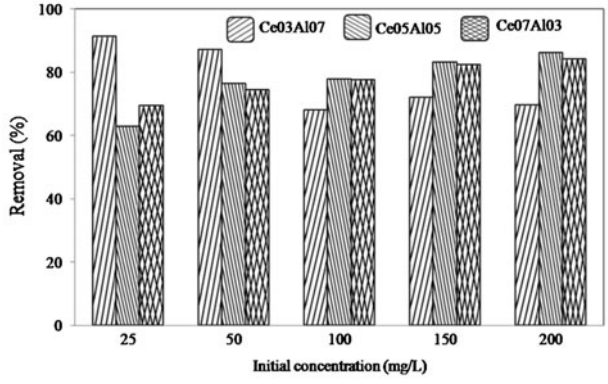

Fig. 8. The effect of initial dye concentration on percentage removal of MV dyes by Ce/Al mixed oxides (adsorbent dose = 0.10 g; pH 9.0).

pore diameter of Ce05Al05 and Ce07Al03 in comparison to Ce03Al07, which implies better diffusivity of MV dye into the pore network system. Moreover, the two adsorbents have higher Ce content, which would lead to formation of more CeO_2 that could provide more binding sites for MV dye at high initial concentration.

3.5. Adsorption isotherm modeling

Equilibrium studies are essential in evaluating the interactive behavior between the contaminant and adsorbent. Moreover, it is fundamental in investigating the adsorption mechanism and designing adsorption systems [44]. In this study, isotherm experimental data were analyzed using Langmuir, Freundlich, and Temkin models.

The Langmuir isotherm model considers the following assumptions: adsorption to occur as a monolayer, adsorption sites are assumed to be energetically equivalent, and no transmigration or interactions among the adsorbed molecules [45–47]. The equation of Langmuir isotherm is represented in Eq. (1):

$$\frac{1}{q_e} = \frac{1}{q_m} + \frac{1}{q_m K_L}\frac{1}{C_e} \tag{1}$$

where q_e is the equilibrium quantity of dye adsorbed onto adsorbent (mg/g), q_m is the maximum monolayer capacity of dye on the adsorbent material (mg/g), and K_L is the adsorption equilibrium constant (L/mg) [19].

The Freundlich isotherm is an empirical equation which has the following assumptions: (1) adsorption occurs on a heterogeneous surface through a multilayered adsorption mechanism with interaction between adsorbed molecules; (2) increase in adsorbate concentration results to an increase in adsorbate concentration on the adsorbent; and (3) applicable for adsorbates at low concentration [46,48–50]. The Freundlich isotherm constants can be calculated using the logarithmic form as shown in Eq. (2):

$$\ln q_e = \ln K_F + \frac{1}{n}\ln C_e \tag{2}$$

where K_F (mg/g) and n are the Freundlich constants associated with adsorption capacity and adsorption intensity of the dye onto the adsorbent, respectively.

The Temkin isotherm describes that the heat of adsorption decreases linearly with layer coverage due to the interaction between the adsorbate and binding sites. The isotherm is also based on the assumption that there is uniform distribution of binding energies up to a certain maximum binding energy [46,50,51]. The Temkin isotherm is expressed as Eq. (3):

$$q_e = B\ln A + B\ln C_e \tag{3}$$

where A is the equilibrium constant corresponding to the maximum binding energy (L/g), and B is the Temkin constant related to the heat of adsorption (kJ/mol) [46].

The computed values of the correlation coefficients and isotherm constants are given in Table 2.

Results obtained show that the adsorption data for Ce03Al07 could be best described by the Langmuir isotherm ($R^2 = 0.9739$), providing q_m of 25.38 mg/g and K_L of 0.13 L/mg. This implies that the adsorption of MV onto Ce03Al07 proceeds by monolayer formation. On the other hand, the Langmuir adsorption parameters have negative q_m and K_L values for Ce05Al05 and Ce07Al03. This implies the inadequacy of the Langmuir model in explaining the adsorption of MV dye onto Ce05Al05 and Ce07Al03, even though an acceptable linearity exists in comparison to Freundlich and Temkin models. Similar results where isotherm parameters have negative values have also been documented by previous studies [46,51,52].

The adsorption data for Ce05Al05 and Ce07Al03 could be best fitted with the Freundlich isotherm with R^2 of 0.9581 and 0.9894, respectively. This indicates that the adsorption of MV onto Ce05Al05 and Ce07Al03 proceeds by multilayer adsorption, signifying that the MV dye is adsorbed onto different binding sites such as Ce–OH, Al–OH, and Ce–O–Al. Although all samples showed only the phase of CeO_2 from FT-Raman results, a suspension of mixed oxide in the dye solution during adsorption may cause

Table 2
Isotherm model parameters obtained for MV adsorption onto Ce03Al07, Ce05Al05, and Ce07Al03

		Adsorbents		
Isotherms	Parameters	Ce03Al07	Ce05Al05	Ce07Al03
Langmuir	q_m (mg/g)	25.38	−11.39	−23.81
	K_L (L/mg)	0.13	−0.03	−0.02
	R^2	0.9739	0.9025	0.9980
Freundlich	K_F (mg/g)	3.91	0.07	0.18
	n (g/L)	2.06	0.53	0.65
	R^2	0.9569	0.9581	0.9894
Temkin	B (kJ/mol)	6.65	28.56	23.97
	A (L/g)	0.89	0.12	0.14
	R^2	0.8615	0.8516	0.8420

Table 3
Comparative adsorption capacities of MV dye onto various adsorbents

Adsorbents	Adsorption capacity of MV dye (mg/g)	T (℃)	References
Granular activated carbon	95.00	25	[20]
Bagasse fly ash	26.24	30	[21]
Mansonia wood sawdust	16.11	26	[22]
Sepiolite	10.24	60	[23]
Unfunctionalized cellulose	43.67	25	[24]
Functionalized cellulose	106.67	25	[24]
Peach gum	277.00	25	[25]
Nanographite/Fe_3O_4	144.72	25	[26]
Ce03Al07	25.28	25	This study

formation of hydrous metal oxide and further adsorb dye molecules. In addition, the Freundlich parameter n indicates the favorability of the MV dye adsorption onto Ce/Al mixed oxide. If $n < 1$, it implies the adsorption intensity is good or favorable in the entire concentration range studied, while $n > 1$ indicates the adsorption intensity is favorable at high concentrations and less at lower concentrations [53]. From the results, the adsorption intensity is good over high initial concentrations for Ce03Al07. Meanwhile, adsorption of MV dye onto Ce05Al05 and Ce07Al03 implies adsorption intensity is good in the entire concentration range studied.

In Table 3, the adsorption capacity of Ce03Al07 in removing MV dye was compared to other adsorbents in previous researches. The Ce03Al07 showed comparable adsorption capacity against bagasse fly ash. Moreover, it exhibited higher capacity for MV adsorption in comparison to mansonia wood sawdust and sepiolite. However, the result of this study has lower capacity in comparison to granular activated carbon, unfunctionalized and functionalized cellulose, peach gum, and nanographite/Fe_3O_4. This implies that the Ce03Al07 is a promising material and has the potential in removing MV dye from aqueous solutions.

4. Conclusion

In the present study, samples of mesoporous Ce/Al oxides (Ce03Al07, Ce05Al05, and Ce07Al03) with different molar ratios via co-precipitation method were successfully prepared. The adsorbents Ce03Al07, Ce05Al05, and Ce07Al03 are characterized by their rough textures and high surface areas, which make it an attractive adsorbent and increase its potential for commercial-scale applications in removing MV dye residues. The maximum adsorption capacity and percent removal were attained at a contact time of 120 min, solution pH of 9.0, and adsorbent dose of 0.10 g. The Langmuir isotherm model provides the best fit for the adsorption behavior of MV dye onto Ce03Al07, yielding a maximum adsorption capacity of 25 mg/g. On the other hand, the Freundlich model best describes the MV dye adsorption onto Ce05Al05 and Ce07Al03.

Acknowledgments

The authors would like to acknowledge the Department of Chemistry, Faculty of Science, Udon Thani Rajabhat University, Thailand, for the financial support provided for this research. Many thanks to Mr Ian James Riach of Health Science Program, Faculty of Science, Udon Thani Rajabhat University for his assistance in proofreading the manuscript.

References

[1] A. Mittal, V. Gajbe, J. Mittal, Removal and recovery of hazardous triphenylmethane dye, Methyl Violet through adsorption over granulated waste materials, J. Hazard. Mater. 150 (2008) 364–375.
[2] R.D. Lillie, H.J. Conn, H.J. Conn's Biological Stains: A Handbook on the Nature and Uses of the Dyes Employed in the Biological Laboratory, Williams and Wilkins, Baltimore, MD, 1977.
[3] W. Au, S. Pathak, C.J. Collie, T.C. Hsu, Cytogenetic toxicity of gentian violet and crystal violet on mammalian cells *in vitro*, Mutat. Res. Genet. Toxicol. 58 (1978) 269–276.
[4] A. Vachálková, L. Novotný, M. Blesová, Polarographic reduction of some triphenylmethane dyes and their potential carcinogenic activity, Neoplasma 43 (1996) 113–117.
[5] B.H. Hameed, A.A. Ahmad, Batch adsorption of methylene blue from aqueous solution by garlic peel, an agricultural waste biomass, J. Hazard. Mater. 164 (2009) 870–875.
[6] B. Royer, N.F. Cardoso, E.C. Lima, T.R. Macedo, C. Airoldi, Sodic and acidic crystalline lamellar magadiite adsorbents for the removal of methylene blue from aqueous solutions: Kinetics and equilibrium studies, Sep. Sci. Technol. 45 (2010) 129–141.
[7] D.H. Ahn, W.S. Chang, T.I. Yoon, Dyestuff wastewater treatment using chemical oxidation, physical adsorption and fixed bed biofilm process, Process Biochem. 34 (1999) 429–439.
[8] F. Deniz, Adsorption properties of low-cost biomaterial derived from *Prunus amygdalus* L. for dye removal from water, Sci. World J. 2013 (2013) 1–8.
[9] F. Banat, S. Al-Asheh, L. Al-Makhadmeh, Evaluation of the use of raw and activated date pits as potential adsorbents for dye containing waters, Proc. Biochem. 39 (2003) 193–202.

[10] V.K. Gupta, Suhas, Application of low-cost adsorbents for dye removal—A review, J. Environ. Manage. 90 (2009) 2313–2342.
[11] R. Jain, P. Sharma, S. Sikarwar, J. Mittal, D. Pathak, Adsorption kinetics and thermodynamics of hazardous dye Tropaeoline 000 unto Aeroxide Alu C (Nano alumina): A non-carbon adsorbent, Desalin. Water Treat. 52 (2014) 7776–7783.
[12] J. Mittal, V. Thakur, A. Mittal, Batch removal of hazardous azo dye Bismark Brown R using waste material hen feather, Ecol. Eng. 60 (2013) 249–253.
[13] H. Daraei, A. Mittal, M. Noorisepehr, J. Mittal, Separation of chromium from water samples using eggshell powder as a low-cost sorbent: Kinetic and thermodynamic studies, Desalin. Water Treat. 53 (2015) 214–220.
[14] H. Daraei, A. Mittal, M. Noorisepehr, F. Daraei, Kinetic and equilibrium studies of adsorptive removal of phenol onto eggshell waste, Environ. Sci. Pollut. Res. 20 (2013) 4603–4611.
[15] H. Daraei, A. Mittal, J. Mittal, H. Kamali, Optimization of Cr(VI) removal onto biosorbent eggshell membrane: Experimental and theoretical approaches, Desalin. Water Treat. 52 (2014) 1307–1315.
[16] J. Mittal, D. Jhare, H. Vardhan, A. Mittal, Utilization of bottom ash as a low-cost sorbent for the removal and recovery of a toxic halogen containing dye eosin yellow, Desalin. Water Treat. 52 (2014) 4508–4519.
[17] A. Mittal, V. Thakur, J. Mittal, H. Vardhan, Process development for the removal of hazardous anionic azo dye Congo red from wastewater by using hen feather as potential adsorbent, Desalin. Water Treat. 52 (2014) 227–237.
[18] G. Sharma, M. Naushad, D. Pathania, A. Mittal, G.E. El-desoky, Modification of *Hibiscus cannabinus* fiber by graft polymerization: Application of dye removal, Desalin. Water Treat. 52 (2014) 1–8.
[19] K. Elass, A. Laachach, A. Alaoui, M. Azzi, Removal of methyl violet from aqueous solution using a stevensite-rich clay from Morocco, Appl. Clay Sci. 54 (2011) 90–96.
[20] S. Azizian, M. Haerifar, H. Bashiri, Adsorption of methyl violet onto granular activated carbon: Equilibrium, kinetics and modeling, Chem. Eng. J. 146 (2009) 36–41.
[21] I.D. Mall, V.C. Srivastava, N.K. Agarwal, Removal of Orange-G and Methyl Violet dyes by adsorption onto bagasse fly ash—Kinetic study and equilibrium isotherm analyses, Dyes Pigm. 69 (2006) 210–223.
[22] A.E. Ofomaja, Kinetic study and sorption mechanism of methylene blue and methyl violet onto mansonia (*Mansonia altissima*) wood sawdust, Chem. Eng. J. 143 (2008) 85–95.
[23] Y. Özdemir, M. Doğan, M. Alkan, Adsorption of cationic dyes from aqueous solutions by sepiolite, Microporous Mesoporous Mater. 96 (2006) 419–427.
[24] S.M. Musyoka, H. Mittal, S.B. Mishra, J.C. Ngila, Effect of functionalization on the adsorption capacity of cellulose for the removal of methyl violet, Int. J. Biol. Macromol. 65 (2014) 389–397.
[25] L. Zhou, J. Huang, B. He, F. Zhang, H. Li, Peach gum for efficient removal of methylene blue and methyl violet dyes from aqueous solution, Carbohydr. Polym. 101 (2014) 574–581.
[26] C. Li, Y. Dong, J. Yang, Y. Li, C. Huang, Modified nano-graphite/Fe_3O_4 composite as efficient adsorbent for the removal of methyl violet from aqueous solution, J. Mol. Liq. 196 (2014) 348–356.
[27] K. Biswas, K. Gupta, U.C. Ghosh, Adsorption of fluoride by hydrous iron(III)–tin(IV) bimetal mixed oxide from the aqueous solutions, Chem. Eng. J. 149 (2009) 196–206.
[28] C. Klett, A. Barry, I. Balti, P. Lelli, F. Schoenstein, N. Jouini, Nickel doped zinc oxide as a potential sorbent for decolorization of specific dyes, methyl orange and tartrazine by adsorption process, J. Environ. Chem. Eng. 2 (2014) 914–926.
[29] M. Szlachta, N. Chubar, The application of Fe–Mn hydrous oxides based adsorbent for removing selenium species from water, Chem. Eng. J. 217 (2013) 159–168.
[30] M. Chen, Y. Zhu, X. Zheng, A novel material of $Ce_{0.7}Zr_{0.3}Ba_{0.1}O_{2.1}$: Synthesis, characterization and its catalytic performance for CO oxidation, Mater. Chem. Phys. 92 (2005) 43–47.
[31] R.C. Deus, C.R. Foschini, B. Spitova, F. Moura, E. Longo, A.Z. Simões, Effect of soaking time on the photoluminescence properties of cerium oxide nanoparticles, Ceram. Int. 40 (2014) 1–9.
[32] Y. Peng, K. Li, J. Li, Identification of the active sites on CeO_2–WO_3 catalysts for SCR of NO_x with NH_3: An *in situ* IR and Raman spectroscopy study, Appl. Catal., B 140–141 (2013) 483–492.
[33] N. Krishna Chandar, R. Jayavel, Synthesis and characterization of C14TAB passivated cerium oxide nanoparticles prepared by co-precipitation route, Phys. E 58 (2014) 48–51.
[34] H. Liu, S. Deng, Z. Li, G. Yu, J. Huang, Preparation of Al–Ce hybrid adsorbent and its application for defluoridation of drinking water, J. Hazard. Mater. 179 (2010) 424–430.
[35] F. Rouquerol, J. Rouquerol, K. Sing, Adsorption by Powders and Porous Solids, Academic Press, London, 1999.
[36] Z. Jia, K. Peng, L. Xu, Preparation, characterization and enhanced adsorption performance for Cr(VI) of mesoporous $NiFe_2O_4$ by twice pore-forming method, Mater. Chem. Phys. 136 (2012) 512–519.
[37] T.Y. Ma, J.L. Cao, G.S. Shao, X.J. Zhang, Z.Y. Yuan, Hierarchically structured squama-like cerium-doped titania: Synthesis, photoactivity, and catalytic CO oxidation, J. Phys. Chem. C 113 (2009) 16658–16667.
[38] A.E. Ofomaja, Y.S. Ho, Effect of temperatures and pH on methyl violet biosorption by Mansonia wood sawdust, Bioresour. Technol. 99 (2008) 5411–5417.
[39] R.K. Xu, S.C. Xiao, J.H. Yuan, A.Z. Zhao, Adsorption of methyl violet from aqueous solutions by the biochars derived from crop residues, Bioresour. Technol. 102 (2011) 10293–10298.
[40] A. Kamari, W.S. Ngah, Isotherm, kinetic and thermodynamic studies of lead and copper uptake by H_2SO_4 modified chitosan, Colloids Surf., B. 73 (2009) 257–266.
[41] C.M. Futalan, C.C. Kan, M.L. Dalida, K.J. Hsien, C. Pascua, M.W. Wan, Comparative and competitive adsorption of copper, lead and nickel using chitosan immobilized on bentonite, Carbohydr. Polym. 83 (2011) 528–536.

[42] S. Chen, J. Zhang, C. Zhang, Q. Yue, Y. Li, C. Li, Equilibrium and kinetic studies of methyl orange and methyl violet adsorption on activated carbon derived from *Phragmites australis*, Desalination 252 (2010) 149–156.
[43] S. Ghorai, A. Sarkar, M. Raoufi, A.B. Panda, H. Schönherr, S. Pal, Enhanced removal of methylene blue and methyl violet dyes from aqueous solution using a nanocomposite of hydrolyzed polyacrylamide grafted xanthan gum and incorporated nanosilica, ACS. Appl. Mater. Interfaces 6 (2014) 4766–4777.
[44] A. Rodríguez, J. García, G. Ovejero, M. Mestanza, Adsorption of anionic and cationic dyes on activated carbon from aqueous solutions: Equilibrium and kinetics, J. Hazard. Mater. 172 (2009) 1311–1320.
[45] R. Liu, B. Zhang, D. Mei, H. Zhang, J. Liu, Adsorption of methyl violet from aqueous solution by halloysite nanotubes, Desalination 268 (2011) 111–116.
[46] M. Alshabanat, G. Alsenani, R. Almufarij, Removal of crystal violet dye from aqueous solutions onto date palm fiber by adsorption technique, J. Chem. 2013 (2013) 1–6.
[47] L. Wang, J. Li, Y. Wang, L. Zhao, Q. Jiang, Adsorption capability for Congo red on nanocrystalline MFe_2O_4 (M=Mn, Fe, Co, Ni) spinel ferrites, Chem. Eng. J. 181–182 (2012) 72–79.
[48] F. Del Rey-Bueno, J. Romero-Carballo, E. Villafranca-Sanchez, A. Garcia-Rodriguez, E.N. Sebastian-Pardo, Adsorption of ammonia over halloysite activated at different temperatures, Mater. Chem. Phys. 21 (1989) 67–84.
[49] K.M. Parida, S. Sahu, K.H. Reddy, P.C. Sahoo, A Kinetic, thermodynamic, and mechanistic approach toward adsorption of methylene blue over water-washed manganese nodule leached residues, Ind. Eng. Chem. Res. 50 (2011) 843–848.
[50] I.A.W. Tan, A.L. Ahmad, B.H. Hameed, Adsorption of basic dye on high-surface-area activated carbon prepared from coconut husk: Equilibrium kinetic and thermodynamic studies, J. Hazard. Mater. 154 (2008) 337–346.
[51] B. Inbaraj, C.P. Chiu, Y.T. Chiu, G.H. Ho, J. Yang, B.H. Chen, Effect of pH on binding of mutagenic heterocyclic amines by the natural biopolymer poly(γ-glutamic acid), J. Agric. Food Chem. 54 (2006) 6452–6459.
[52] S.M. Ragheb, Phosphate removal from aqueous solution using slag and fly ash, Hous. Build. Natl. Res. Ctr. J. 9 (2013) 270–275.
[53] W.S. Ngah, S. Fatinathan, Adsorption of Cu(II) ions in aqueous solution using chitosan beads, chitosan-GLA beads and chitosan-alginate beads, Chem. Eng. J. 143 (2008) 62–72.